Journal of Molecular Spectroscopy 390 (2022) 111718

Contents lists available at ScienceDirect

Journal of Molecular Spectroscopy

journal homepage: www.elsevier.com/locate/yjmsp

Synchrotron-based infrared spectroscopy of the Coriolis perturbed ν_6 and ν_8 bands of *trans*-DCOOH

Lauren Slaber [c], Jianbao Zhao [a], Brant E. Billinghurst [a], Paul L. Raston [b,c,*]

[a] Canadian Light Source Inc., 44 Innovation Boulevard, Saskatoon, Saskatchewan S7N 2V3, Canada
[b] Department of Chemistry, University of Adelaide, SA 5005, Australia
[c] Department of Chemistry and Biochemistry, James Madison University, Harrisonburg, VA 22807, United States

ARTICLE INFO

Keywords:
PGOPHER
Infrared spectroscopy
Formic acid
Perturbations

ABSTRACT

Previously, the Coriolis perturbed ν_6 and ν_8 bands of *trans*-DCOOH were analysed using a high-resolution infrared spectrum that only contained lines from the ν_6 fundamental; the ν_8 fundamental was too weak to be directly observed [Goh *et al.*, *Spectrochim. Acta A: Mol. Biomol. Spectrosc.* **1999**, *55*, 1309]. Using a long pathlength multireflection cell and highly brilliant synchrotron radiation, we were able to observe the ν_8 fundamental with excellent signal-to-noise (in addition to the ν_6 fundamental). Analysis of the spectra using PGOPHER and SPFIT resulted in determination of an extensive set of molecular parameters, including two *a*-axis and four *b*-axis Coriolis coupling constants. The set features a significant refinement of the $\nu_8 = 1$ constants, with a band origin at 873.3848785(83) cm^{-1}, which is ~ 0.72 cm^{-1} higher than previously determined.

1. Introduction

Along with acetic acid, formic acid is the most abundant organic acid in both the Earth's atmosphere [1], and in interstellar molecular clouds [2]. In the atmosphere, it plays a major role in the acidification of rain [3], especially in the tropics [4], and in the interstellar medium (ISM) it is thought to play an important role in the chemistry that leads to the formation of Complex Organic Molecules (COMs) [5], i.e., organic molecules that contain six or more atoms [6]. Since its first detection in the ISM, towards Sagittarius B2 [7], formic acid has been detected towards a variety of different sources, including the hot molecular core in Orion-KL [8], the dark molecular cloud, L134N [9], and the protoplanetary disk around TW Hydrae [10]. All of those observations were of *trans*-HCOOH, which is ~ 3.9 kcal/mol more stable than *cis*-HCOOH [11]. The higher energy *cis* rotamer has since been observed in the ISM towards the UV irradiated edge of the Orion Bar [12], with a similar abundance to the *trans* rotamer [13]. The abundance of the minor isotopologues of *trans*-formic acid are much lower in the ISM [14]. While both HCOOD and DCOOH were tentatively detected in a molecular line survey over 30 years ago [15], it wasn't until recently that these detections were confirmed (along with the observation of $H^{13}COOH$) [14].

It is becoming increasingly more important to characterize molecules that have been detected in the ISM, in vibrationally excited states. This is on account of increasingly more sensitive radio-telescopes such as the Atacama Large Millimeter/submillimeter Array (ALMA), the survey spectra from which contain a large fraction of unidentified lines; for example, ~40 % of lines observed towards the Barnard 1b core were reported as unidentified in a recent ALMA Band 6 spectral line survey [16]. Far-infrared synchrotron-based spectroscopy is well suited to help characterize astrophysically relevant molecules in vibrationally excited states, and accordingly, there has been a surge in the number of such molecules that have been investigated by this technique, e.g., vinyl acetylene [17], vinyl alcohol [18], acetone [19], ethyl cyanide [20], methanol [21], phenol [22], aminoacetonitrile [23], glycolaldehyde [24], 2-chloroethanol [25], and benzonitrile [26]. The focus of this article is on the synchrotron-based high-resolution infrared spectrum of the important interstellar molecule, *trans*-DCOOH, around 11 μm.

The band origins of all the fundamentals of *trans*-DCOOH have been determined, to varying degrees of accuracy by FTIR and Raman spectroscopies. The two lowest frequency fundamentals [ν_7 (OCO scissor at ~ 621 cm^{-1}) and ν_9 (COH torsion at ~ 632 cm^{-1})] are strongly Coriolis perturbed, and have been directly observed and extensively analyzed via FTIR spectroscopy [27]. The next two higher frequency fundamentals are ν_8 (DCO torsion at ~ 873 cm^{-1}) and ν_6 (CD rocking at ~ 971 cm^{-1}), which are also Coriolis perturbed, but to a much lesser extent owing to the 10x greater separation between the excited states. Goh *et al.* directly

* Corresponding author.
E-mail address: rastonpl@jmu.edu (P.L. Raston).

https://doi.org/10.1016/j.jms.2022.111718
Received 30 September 2022; Received in revised form 15 November 2022; Accepted 16 November 2022
Available online 21 November 2022

observed the ν_6 fundamental, and in their analysis, they not only determined spectroscopic parameters for $\nu_6 = 1$, but also the band origin of the interacting $\nu_8 = 1$ dark state [28]. The remaining fundamentals all have band origins above 1000 cm^{-1}, i.e., ν_5 at ~ 1142 cm^{-1} [29], ν_4 at 1299 cm^{-1} [30], ν_3 at 1762 cm^{-1} [31], ν_2 at ~ 2220 cm^{-1} [32], and ν_1 at 3566 cm^{-1} [33]. In the following, we report an investigation of the Coriolis perturbed ν_6 and ν_8 bands of *trans*-DCOOH. In the original work, Goh *et al.* used a single pass cell (0.2 m pathlength) coupled to a Bomem FTIR spectrometer with an unapodized resolution of 0.0024 cm^{-1}. Here, we used a multipass cell (72 m total pathlength) coupled to a Bruker FTIR spectrometer with an unapodized resolution that is ~ 3x "higher" (0.00096 cm^{-1}). This allowed for the determination of more accurate line positions, in addition to the first direct observation of the very weak ν_8 fundamental.

2. Experimental

The high-resolution infrared spectra of DCOOH were acquired at the Canadian Light Source using a similar setup to what we previously used for the normal isotopologue of formic acid [34]. In brief, we introduced 4–64 mTorr of DCOOH (Millipore-Sigma) into a 2 m long White cell (at 333 K) that was optimized for 36 passes [35]. The cell is housed in a Bruker IFS 125 HR FTIR spectrometer that was equipped with optics well suited for covering the 400–1250 cm^{-1} range, where the synchrotron advantage is active [36]. This included utilizing a KBr beamsplitter and windows, and a Ge:Cu detector within a pulsed-tube cryocooler. Spectra of the analyte were recorded at maximum resolution and ratioed against a lower resolution reference spectrum that was collected with an evacuated cell to give absorbance spectra, $A(\bar{\nu}) = \log[I_0(\bar{\nu})/I(\bar{\nu})]$, which is analyzed in the following.

3. Analysis and discussion

Trans-DCOOH is a planar, near prolate top [asymmetry parameter $\kappa = (2B\text{-}A\text{-}C)/(A\text{-}C) = -0.912$], which belongs to the C_s point group. It has 9 vibrational modes, 5 of which fall in the 400–1250 cm^{-1} range of the spectrometer, as shown in Fig. 1. The central Q branch of both the ν_6 and much weaker ν_8 fundamentals are evident at this relatively low pressure (4 mTorr) spectrum, although the signal-to-noise of the latter (ν_8) is very low. The ν_8 fundamental with an a'' symmetry upper vibrational state is a c-type band with rotational selection rules, ΔK_a = odd, ΔK_c = even. This gives rise to the relatively narrow central ${}^pQ_1/{}^rQ_0$ bandhead which is shown in Fig. 2. The ν_6 fundamental, on the other hand, has an a' upper vibrational state, which results in a hybrid a/b-type band with rotational selection rules, ΔK_a = even, ΔK_c = odd for a-type transitions, and ΔK_a = odd, ΔK_c = odd for b-type transitions. The a-type component of this band gives rise to the central Q branch which is shown in Fig. 3. The simulated spectra that are shown throughout were generated using PGOPHER, which was also used to make line assignments, identify Coriolis interactions, and perform initial fits that are described in the following [37]. Throughout, we utilized Watson's A-reduced Hamiltonian in the I^r representation [38].

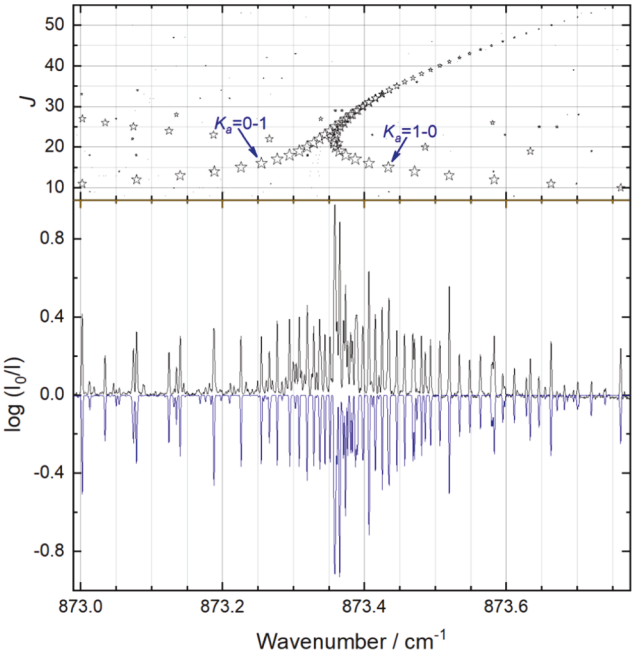

Fig. 2. Illustration of the central Q branch of the ν_8 fundamental of *trans*-DCOOH (lower panel), and associated Fortrat diagram (upper panel). The cell pressure was 64 mTorr. In the lower panel, the experimental spectrum is shown in black while the simulated spectrum (inverted) is shown in blue.

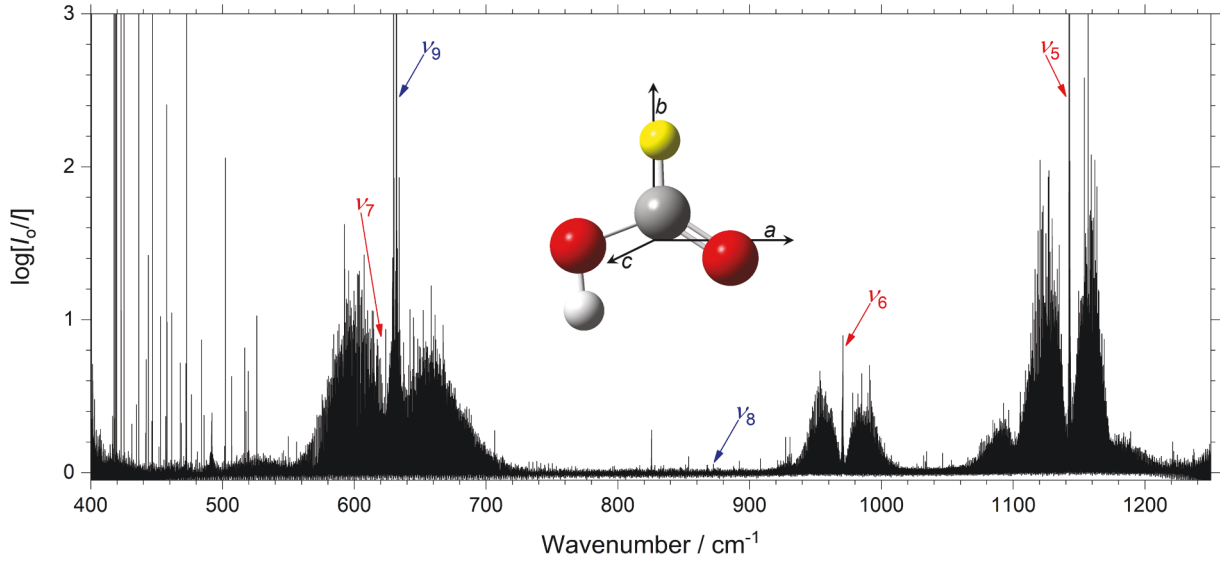

Fig. 1. Survey spectrum of DCOOH at a cell pressure of 4 mTorr. Fundamental band origins of the *trans* rotamer are arrowed in red [blue] for a' [a''] symmetry vibrations. The inset shows the inertial axes superimposed on the MP2/aug-cc-pVTZ optimized structure of *trans*-formic acid; the a- and b-axes are in-plane.

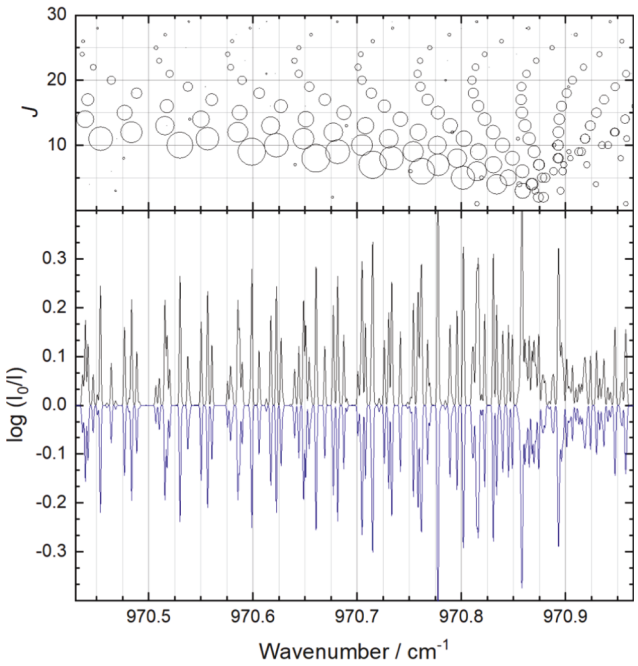

Fig. 3. The central Q branch of the ν_6 fundamental of *trans*-DCOOH (lower panel). Symbols in the associated Fortrat diagram have been reduced in magnitude by 198x in comparison to what is shown for the ν_6 fundamental (198 is the ratio of calculated anharmonic band intensities). The cell pressure was 4 mTorr.

The fitting process was begun by simulating the spectrum of the ν_6 and ν_8 fundamentals utilizing the ground and excited state parameters listed in Table 1 of Ref. [28]. While we found good agreement between the simulated and experimental spectrum (at low K_a) in the ν_6 fundamental, it was poor in the ν_8 fundamental. After assigning > 1000 lines in ν_6 we shifted the band origin of ν_8 up by ~ 0.8 cm^{-1}, and after several attempts of increasing or decreasing the J value assignments in the central $^{P}Q_1/^{r}Q_0$ bandhead, followed by fitting the band origin and select low order rotational constants, we reached reasonable agreement in this region between the simulated and experimental spectrum. It was then possible to make assignments in higher ^{P}Q and ^{r}Q sub-branches, and after a number of iterations involving assigning higher J lines, followed by fitting increasingly higher order constants, we converged upon reasonable agreement between the experimental and simulated spectra in the ν_8 fundamental. The shift of the ν_8 bandorigin up by ~ 0.8 cm^{-1} resulted in much larger residuals in the ν_6 fundamental, which was resolved by floating the first-order Coriolis coupling constants (G_a and G_b), and reassigning a large number of lines in the ν_6 fundamental, especially b-type lines within the broad P and R branch wings (the latter of which significantly overlaps with the P branch of the ν_5 fundamental at high J).

After converging upon a reasonably good agreement between the simulated and experimental spectra, we replaced the ground state constants with the more accurate ones reported in Ref. [39], and included previously reported submillimeter wave lines in the fit [40]. These lines correspond to pure rotational transitions of *trans*-DCOOH in the first excited ν_6 and ν_8 states, which have uncertainty that range from 40 kHz to 1 MHz [40]. We used an uncertainty of 0.00024 cm^{-1} for the infrared lines identified here, which is equal to one-quarter of the unapodized resolution. The inclusion of several higher order Coriolis coupling constants (G_a^J, G_b^J, G_b^K, and G_b^{JJ}) resulted in a significant reduction in the residuals for perturbed lines, such as the $27_{4,24}$–$28_{4,25}$ line in the ν_6 fundamental (see Fig. 4), the upper state of which is in near resonance with the $27_{9,18}$ state within $\nu_8 = 1$. These upper states differ by $\Delta K_a = 5$, and are linked by the b-type Coriolis terms (ΔK_a=±1) that couple states that differ by ΔK_a=±3,±5,….

After completing the preliminary fit of the molecular parameters to the line positions using PGOPHER, the line assignments were exported so that the final fits could be performed using SPFIT [41]. The output from SPFIT was processed with PIFORM in order to assist with data interpretation [42]; the resulting parameters and statistics from which are provided in Table 1. (Please note that these values do not significantly differ from what was gotten using PGOPHER.) We ultimately assigned 11,833 transitions to 8314 lines within the Coriolis perturbed fundamentals of *trans*-DCOOH that we investigated here. Ground state combination differences for each band show excellent agreement with previously reported pure rotational transition frequencies. It is worth noting that the refined band origins are in excellent agreement with the MCTDH (multiconfiguration time-dependent Hartree) calculations of Aerts et al. [43].

Fig. 5 shows a plot of the residuals from the final fit, in comparison to one that was performed where we did not include the Coriolis parameters (from which we omitted significantly perturbed lines). The latter plot reveals a large degree of coupling between the vibrational manifolds, as evidenced by the large residuals between observed and calculated values within a variety of K_a series. Of note in our fit is the inclusion of K_a'=9 and 10 levels at high J that were omitted in the previous analysis "because their line positions were highly displaced" [28]. We were able to include them in our analysis, largely on account of the high brightness of the synchrotron radiation, which allowed for the direct observation of the ν_8 fundamental for the first time. We captured an avoided crossing within the much more intense ν_6 fundamental, the associated lines from which were assigned largely using the higher pressure spectrum (at 64 mTorr). Fig. 6 highlights this avoided crossing

Table 1
Spectroscopic parameters of *trans*-DCOOH determined from the simultaneous analysis of the ν_6 and ν_8 fundamentals. Ground state values (kept fixed in the analysis) are shown for comparison. Parenthetical numbers indicate uncertainty (1σ error) in the last two digits.

Parameter	Ground state[a]	DCO torsion (ν_8)	CD rock (ν_6)
Band origin			
ν_0 (cm^{-1})		873.3848785(83)[b]	970.8889931(77)[b]
Rotational constants			
A (MHz)	57709.22064(49)	57465.199(15)	57596.446(14)
B (MHz)	12055.978611(24)	12044.805(20)	12061.157(19)
C (MHz)	9955.609676(24)	9962.82935(99)	9944.04908(68)
Quartic centrifugal distortion constants			
Δ_J (kHz)	9.440282(99)	9.6959(21)	9.6044(21)
Δ_{JK} (kHz)	−39.59550(12)	−34.865(14)	−39.597(13)
Δ_K (kHz)	757.831(11)	734.259(33)	752.037(13)
δ_J (kHz)	2.2260314(54)	2.3433(11)	2.25735(99)
δ_K (kHz)	37.55853(92)	35.472(26)	39.710(12)
Sextic centrifugal distortion constants			
Φ_J (Hz)	0.01221(18)	0.00863(16)	[c]
Φ_{JK} (Hz)	0.1751(10)	[c]	0.2482(75)
Φ_{KJ} (Hz)	−4.5392(35)	[c]	[c]
Φ_K (Hz)	36.008(84)	[c]	[c]
ϕ_J (Hz)	0.0059633(40)	[c]	[c]
ϕ_{JK} (Hz)	0.0993(11)	[c]	[c]
ϕ_K (Hz)	7.574(29)	[c]	11.47(20)
Octic centrifugal distortion constants			
L_J (mHz)	−0.00022(16)	[c]	[c]
L_{JJK} (mHz)	−0.001793(41)	[c]	[c]
L_{JK} (mHz)	0.00230(32)	[c]	[c]
L_{KKJ} (mHz)	0.2395(23)	[c]	[c]
L_K (mHz)	−11.93(16)	[c]	[c]
l_{JK} (mHz)	0.00144(38)	[c]	[c]
Decic centrifugal distortion constants			
P_J (μHz)	0.000126(61)	[c]	[c]
P_{KKJ} (μHz)	−0.0170(16)	[c]	[c]
Dodecic centrifugal distortion constants			
T_J (nHz)	−0.0000202(81)	[c]	[c]
Coriolis coupling			
G_a (MHz)			2544.8(80)
G_a^J (MHz)			−0.1086(35)
G_b (MHz)			14138.3(20)
G_b^J (MHz)			−0.10658(43)
G_b^K (MHz)			−0.3273(26)
G_b^{JJ} (Hz)			−1.480(10)
Fit summary			
N_{lines}[d]		64 MMW + 3111 IR	50 MMW + 5203 IR
Max. J, K_a		63, 18	77, 27
σ_{ms} MMW (kHz)			79.9
σ_{ms} IR (MHz)			4.21

[a] From Reference [39].
[b] Uncertainty in the band origin does not include calibration error.
[c] Fixed to ground state values.
[d] The rotational lines at 328187.06, 330511.82, 331855.28, 398263.80, 420404.00, and 469064.70 MHz were omitted from the fit because they had unacceptably large residuals [40].

which occurs within a K_a'=10 series in going from $J = 48$ to 49. This series is perturbed by an interaction between K_a'=10 in $\nu_6 = 1$ and K_a'=13 in $\nu_8 = 1$.

4. Summary and outlook

Here, we refined the spectroscopic parameters of the known interstellar molecule, *trans*-DCOOH, by performing a fit to the two Coriolis perturbed bands around 11 μm. While the refined parameters for $\nu_6 = 1$ are similar to those previously reported [28], those for $\nu_8 = 1$ were significantly improved upon. The refined parameters will allow for accurate predictions of pure rotational line positions of vibrationally excited *trans*-DCOOH to be made over a broad range of angular momenta (up to at least $J = 70$ for $\nu_6 = 1$ and $J = 60$ for $\nu_8 = 1$) and frequencies (beyond 2 THz); they should prove useful in radio-astronomical searches of vibrationally warm *trans*-DCOOH. Future work on this molecule involves investigating the ν_4 (1299 cm^{-1} [30]), ν_3 (1762 cm^{-1} [31]), and ν_1 (3566 cm^{-1} [33]) fundamentals by high-resolution infrared spectroscopy, since their band origins are only known to relatively low precision.

CRediT authorship contribution statement

Lauren Slaber: Spectroscopic analysis. **Jianbao Zhao:** Experimentation. **Brant Billinghurst:** Experimentation. **Paul L. Raston:** Conceptualization, Writing – review & editing.

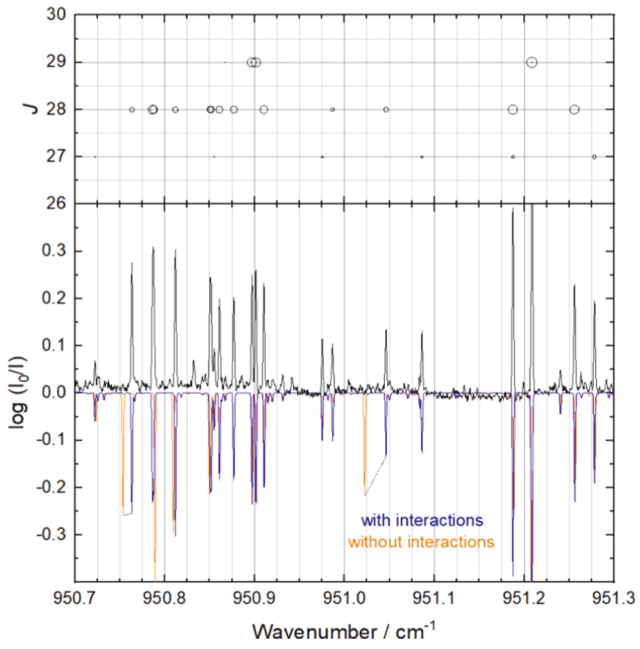

Fig. 4. Illustration of a similar region as shown in Fig. 4 of Ref. [28]. Most of the peaks belong to the *P* branch of the ν_6 fundamental. The cell pressure was 4 mTorr. The blue [orange] simulation was generated using parameters from fits that included [omitted] Coriolis interactions. Dotted lines connect simulated peaks between the fits that share the same sets of quantum numbers (i.e., same transitions; only the two most perturbed pairs are connected).

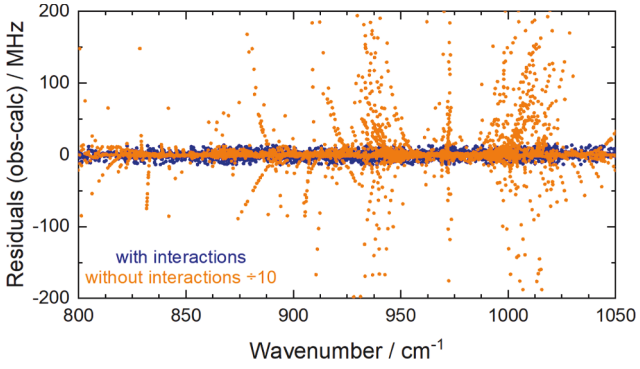

Fig. 5. Residuals in the infrared region from the fits which either included Coriolis interactions (blue) or omitted them (orange; note the residuals were divided by a factor of 10 for clarity).

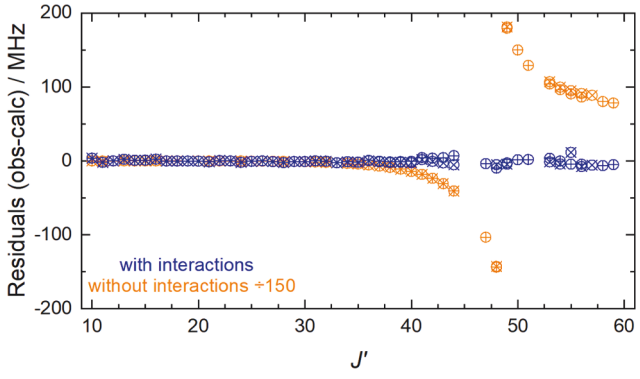

Fig. 6. Close-up of the infrared residuals for K_a'=K_a"=10 transitions. Data points correspond to fits which either included Coriolis interactions (blue) or omitted them (orange; note the residuals were divided by a factor of 150 for clarity).

Declaration of Competing Interest

The authors declare that they have no known competing financial interests or personal relationships that could have appeared to influence the work reported in this paper.

Data availability

Data will be made available on request.

Acknowledgements

Research described in this paper was performed at the Canadian Light Source, which is supported by the Canada Foundation for Innovation, Natural Sciences and Engineering Research Council of Canada, the University of Saskatchewan, the Government of Saskatchewan, Western Economic Diversification Canada, the National Research Council Canada, and the Canadian Institutes of Health Research. Calculations were performed on the supercomputing resources provided by the Phoenix HPC service at the University of Adelaide. Acknowledgement is made to the National Science Foundation (CHE-2141774). We are particularly grateful to the late Colin M. Western for suggesting various approaches for dealing with perturbations in PGOPHER.

Appendix A. Supplementary material

Supplementary data to this article can be found online at https://doi.org/10.1016/j.jms.2022.111718.

References

[1] P. Khare, N. Kumar, K.M. Kumari, S.S. Srivastava, Rev Geophys. 37 (1999) 227.
[2] S. Pilling, L. Baptista, H.M. Boechat-Roberty, D.P. Andrade, Astrobiology 11 (2011) 883.
[3] W. C, Keene, J. N, Galloway, J. D, Holden, JGR: Oceans **88**, 5122 (1983).
[4] S. Eugenio, F. Zoila, R. Johnny, S. Magaly, Ambio 20 (1991) 115.
[5] L. Zamirri, P. Ugliengo, C. Ceccarelli, A. Rimola, ACS Earth Space Chem. 3 (2019) 1499.
[6] E. Herbst, E.F.v. Dishoeck, Annu. Rev. Astron. Astrophys. 47 (2009) 427.
[7] B. Zuckerman, J.A. Ball, C.A. Gottlieb, Astrophys. J. 163 (1971) L41.
[8] S.Y. Liu, D.M. Mehringer, L.E. Snyder, Astrophys. J. 552 (2001) 654.
[9] W.M. Irvine, P. Friberg, N. Kaifu, H.E. Matthews, Y.C. Minh, M. Ohishi, S. Ishikawa, Astron Astrophys 229 (1990) L9.
[10] C. Favre, D. Fedele, D. Semenov, S. Parfenov, C. Codella, C. Ceccarelli, E.A. Bergin, E. Chapillon, L. Testi, F. Hersant, B. Lefloch, F. Fontani, G.A. Blake, L.I. Cleeves, C. Qi, K.R. Schwarz, V. Taquet, Astrophys. J. 862 (2018) L2.
[11] W.H. Hocking, Z. Naturforsch A 31 (1976) 1113.
[12] S. Cuadrado, J.R. Goicoechea, O. Roncero, A. Aguado, B. Tercero, J. Cernicharo, Astron. Astrophys. 596 (2016) L1.
[13] S. Cuadrado, J.R. Goicoechea, J. Cernicharo, A. Fuente, J. Pety, B. Tercero, Astron. Astrophys. 603 (2017) A124.
[14] J.K. Jørgensen, H.S.P. Müller, H. Calcutt, A. Coutens, M.N. Drozdovskaya, K. I. Öberg, M.V. Persson, V. Taquet, E.F. van Dishoeck, S.F. Wampfler, Astron. Astrophys. 620 (2018) A170.
[15] B.E. Turner, Astrophys. J. Suppl. Ser. 70 (1989) 539.
[16] N. Marcelino, M. Gerin, J. Cernicharo, A. Fuente, H.A. Wootten, E. Chapillon, J. Pety, D.C. Lis, E. Roueff, B. Commerçon, A. Ciardi, Astron. Astrophys. 620 (2018) A80.
[17] C.P. Endres, G.C. Mellau, M.E. Harding, M.-A. Martin-Drumel, H. Lichau, S. Thorwirth, J. Mol. Spec. 379 (2021), 111469.
[18] H, Bunn, R, Hudson, A. S, Gentleman, P. L, Raston, ACS Earth Space Chem. (2017). H. Bunn, R. M. Soliday, I. Sumner, and P. L. Raston, Astrophys. J. **847**, 67 (2017). H. Bunn, K. Hull, I. Miller, and P. L. Raston, J. Phys. Chem. A **124**, 704 (2020). H. Bunn, and P. L. Raston, J. Phys. Chem. A **126**, 2569 (2022); note that in the residuals plot (Figure 5), the principal axis values were accidentally divided by k_B (0.695 cm^{-1}/K).
[19] V. Ilyushin, I. Armieieva, O. Dorovskaya, I. Krapivin, E. Alekseev, M. Tudorie, R. A. Motienko, L. Margulès, O. Pirali, E.S. Bekhtereva, S. Bauerecker, C. Maul, C. Sydow, B.J. Drouin, J. Mol. Spec. 363 (2019), 111169.
[20] C.P. Endres, M.-A. Martin-Drumel, O. Zingsheim, L. Bonah, O. Pirali, T. Zhang, Á. Sánchez-Monge, T. Möller, N. Wehres, P. Schilke, M.C. McCarthy, S. Schlemmer, P. Caselli, S. Thorwirth, J. Mol. Spec. 375 (2021), 111392.
[21] R.M. Lees, L.-H. Xu, B.E. Billinghurst, J. Mol. Struct. 1209 (2020), 127960.
[22] S. Albert, P. Lerch, R. Prentner, M. Quack, Angew. Chem. Int. Ed. 52 (2013) 346.
[23] M. Melosso, A. Belloche, M.-A. Martin-Drumel, O. Pirali, F. Tamassia, L. Bizzocchi, R.T. Garrod, H.S.P. Müller, K.M. Menten, L. Dore, C. Puzzarini, Astron. Astrophys. 641 (2020) A160.

[24] B. Collier, K. Krueger, I. Miller, J. Zhao, B.E. Billinghurst, P.L. Raston, Astrophys. J. Suppl. Ser. 253 (2021) 40.
[25] R. M, Soliday, H, Bunn, I, Sumner, P. L, Raston, J. Phys. Chem. A **123**, 1208 (2019). K. Hull, R. M. Soliday, and P. L. Raston, J. Mol. Struct. **1217**, 128369 (2020).
[26] M.A. Zdanovskaia, M.-A. Martin-Drumel, Z. Kisiel, O. Pirali, B.J. Esselman, R. C. Woods, R.J. McMahon, J. Mol. Spec. 383 (2022), 111568.
[27] O.I. Baskakov, J. Lohilahti, V.M. Horneman, J. Mol. Spec. 219 (2003) 191.
[28] K.L. Goh, P.P. Ong, T.L. Tan, H.H. Teo, Spectrochim, Acta, - A: Mol. Biomol. Spectrosc. 55 (1999) 1309.
[29] K.L. Goh, P.P. Ong, T.L. Tan, W.F. Wang, H.H. Teo, J. Mol. Spec. 190 (1998) 125.
[30] A. Nejad, M.A. Suhm, K.A.E. Meyer, Phys. Chem. Chem. Phys. 22 (2020) 25492.
[31] A. Perrin, J. Vander Auwera, Z. Zelinger, J. Quant. Spectrosc. Radiat. Transf. 110 (2009) 743.
[32] T.L. Tan, K.L. Goh, P.P. Ong, H.H. Teo, J. Mol. Spec. 198 (1999) 387.
[33] J.E. Bertie, K.H. Michaelian, H.H. Eysel, D. Hager, J. Chem. Phys. 85 (1986) 4779.
[34] K. Hull, T. Wells, B.E. Billinghurst, H. Bunn, P.L. Raston, AIP Advances 9 (2019), 015021.
[35] J.U. White, J. Opt. Soc. Am. 32 (1942) 285.
[36] A.R.W. McKellar, J. Mol. Spec. 262 (2010) 1.
[37] C.M. Western, J. Quant. Spectrosc. Radiat. Transf. 186 (2017) 221.
[38] J. K. G, Watson, *in: J.R. Durig (Ed.), Vibrational Spectra and Structure, A Series of Advances, vol. 6, Elsevier, New York, 1977 (Chap. 1)*; G. W. King, R. M. Hainer, and P. C. Cross, J. Chem. Phys. **11**, 27 (1943).
[39] G. Cazzoli, C. Puzzarini, S. Stopkowicz, J. Gauss, Astrophys. J. Suppl. Ser. 196 (2011) 10.
[40] O.I. Baskakov, J. Mol. Spec. 180 (1996) 266.
[41] H.M. Pickett, J. Mol. Spec. 148 (1991) 371.
[42] Z, Kisiel, http://www.ifpan.edu.pl/~kisiel/asym/asym.htm#piform (accessed August (2022).
[43] A. Aerts, P. Carbonnière, F. Richter, A. Brown, J. Chem. Phys. 152 (2020), 024305.